Reanalysis of the electrostatic component of the persistence length of poly(styrene sulphonate)*

Kenneth S. Schmitz
Department of Chemistry, University of Missouri–Kansas City, Kansas City, Missouri 64110, USA
(Received 22 November 1989; accepted 3 February 1990)

The electrostatic component of the persistence length (L_{el}) for three molecular-weight preparations of poly(styrene sulphonate) was determined from magnetic birefringence measurements (m.b.m.) by Weill and Maret in 1982. The ratio L_{el}/L^a_{el} plotted as a function of the Debye–Hückel screening length (λ_{DH}) exhibited significant deviations from unity over the range $24 \leqslant \lambda_{DH}$ (Å) $\leqslant 108$, where L^a_{el} is the analytical expression for the electrostatic persistence length for finite chain lengths given by Odijk. Weill, Maret and Odijk attempted to explain the discrepancy between theory and experiment by invoking 'semidilute' solution conditions for the long-chain results concomitant with a different degree of counterion condensation than used for the short-chain results.

It is proposed in the present paper that a 'three-region' model for the counterion distribution about the polyion accurately represents the m.b.m. data without having to invoke differential counterion condensation properties of short and long chains, or having to postulate semidilute solution conditions. The three regions are: (1) Manning-type condensation on the surface of the polyion; (2) a counterion sheath in the vicinity of the polyion; and (3) the remaining solution.

(Keywords: counterion distribution; Debye–Hückel screening)

INTRODUCTION

The concept of a 'persistence length', or 'correlation length', is of value in describing the static and dynamic properties of a flexible polymer. A linear flexible polymer of contour length L can undergo at least three distinct types of motion: (1) stretching and contracting such that the contour length fluctuates by $\pm dL$; (2) bending through an angle θ defined by the deviation from a rod-like configuration; and (3) twisting through an angle ω about the equilibrium configuration about the long axis of the polymer.

The focus of the present study is on the ionic strength dependence of L_b, the persistence length of bending. The local stiffness approximation (small deviations from rod-like extension on the microscopic scale) allows one to write:

$$L_b = L_{in} + L_{el} \tag{1}$$

where L_{in} is the so-called 'intrinsic part' of L_b and L_{el} is the 'electrostatic component' of L_b that is responsive to the electrical environment of the solution. For a chain of finite length in the rod-like limit, Odijk[1] obtained the following *analytical* expression for L_{el} (denoted as L^a_{el} and referred to as the analytical model):

$$L^a_{el} = (\lambda_B \lambda^2_{DH}/4\langle b_{eff}\rangle^2) h(L/\lambda_{DH}) \tag{2}$$

where $1/\langle b_{eff}\rangle$ is the average linear charge density, λ_{DH} is the usual Debye–Hückel screening length, given by:

$$\lambda_{DH} = (1000/8\pi N_A \lambda_B I_s)^{1/2} \tag{3}$$

N_A is Avogadro's number, I_s is the ionic strength in moles/litre, $\lambda_B = e^2/\varepsilon kT$ is the Bjerrum length (e is the proton charge, ε is the bulk dielectric constant, and kT is the thermal energy), and:

$$h(Y) = 1 - (8/3Y) + [\exp(-Y)/3][Y + 5 + (8/Y)] \tag{4}$$

accounts for the finite length of the chain. Note that for $h(\infty) = 1$, equation (2) reduces to the series expansion result of Skolnick and Fixman[2] for a chain of infinite length whose configuration deviates slightly from a rod.

Manning[3–5] has suggested that counterions condense onto charged rods (or cylinders) whose charged groups are separated by a distance b if:

$$Z_c \xi_M > 1 \tag{5}$$

where Z_c is the counterion charge and $\xi_M = \lambda_B/b$ is the Manning condensation parameter. The physical significance of equation (5) is that the solvent cannot support a linear charge density greater than $1/\lambda_B$. Counterions will therefore condense onto the surface until the condition $\langle b_{eff}\rangle = b/Z_c = \lambda_B$ is met. Odijk and Houwaart[6] modified equation (2) to include Manning condensation by an *ad hoc* substitution of $\lambda_B = \langle b_{eff}\rangle$.

Weill and Maret reported magnetic birefringence data on poly(styrene sulphonate) (PSS)[7] and deoxyribonucleic acid (DNA)[8]. The ionic strength of these solutions was computed from the relationship:

$$I_s = C_s + (\alpha/2)C_p \tag{6}$$

where C_s is the concentration of added 1:1 electrolyte, α is the degree of ionization of the polyion, and C_p is the monomer concentration of the polyion. These authors assumed that $h(y) = 1$ in their use of equation (2).

* Dedicated to Professor Walther Burchard on the occasion of his 60th birthday

0032-3861/90/101823-08

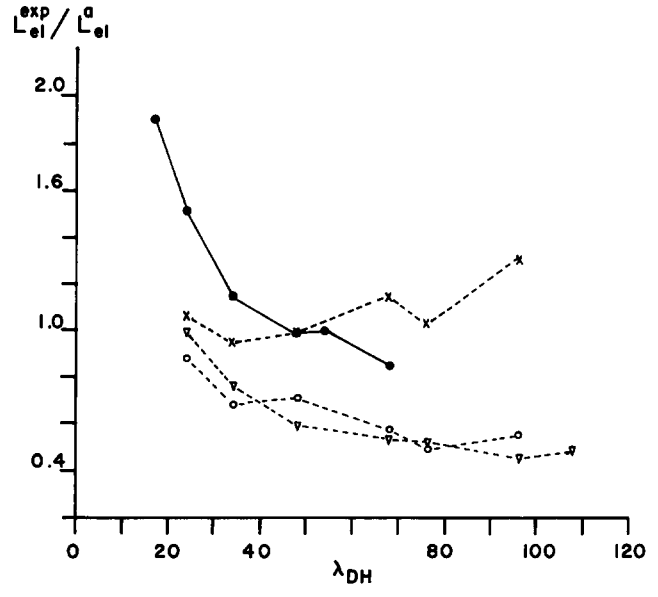

Figure 1 L_{el}^{exp}/L_{el}^{a} *versus* λ_{DH} for poly(styrene sulphonate). Magnetic birefringence measurements were used by Weill and Maret[7] to study the ionic strength dependence of L_{el} for PSS. The above data were obtained for the following ionic strength assumptions: $I_s=0.18C_p$ ($MW=15000$ (×), 40000 (▽), 140000 (○)); and $I_s=0.36C_p$ ($MW=140000$ (●))

Reasonable agreement between the experimental and theoretical values of L_b was obtained for DNA using $L_{in}=50$ nm in equation (1) and Manning condensation ($\alpha=0.24$) in equation (2). However, the results on the PSS system ($L_{in}=1.2$ nm and $\alpha=0.36$) were not as encouraging as in the DNA analysis.

Weill, Maret and Odijk[9] reanalysed the PSS data in the absence of added salt ($I_s=(\alpha/2)C_p$) using the full expression of equation (2). The results in their table 1 are plotted as L_{el}^{exp}/L_{el}^{a} *versus* λ_{DH} in *Figure 1* for $I_s=0.18C_p$ and $I_s=0.36C_p$, where L_{el}^{exp} is the experimental value of the electrostatic persistence length.

Weill *et al.*[9] noted that the Manning condensation condition ($I_s=0.18C_p$) gave reasonable agreement between L_{el}^{a} and L_{el}^{exp} *only for the shortest chain length.* The question is therefore raised as to the validity of either Manning condensation *for flexible chains* or the analytical expression for L_{el}^{a}, or both models. Apparently these authors chose to retain the analytical expression for L_{el}^{a} *in the dilute solution limit*, which necessitated the relationship $I_s=0.36C_p$ to fit the experimental data for the higher molecular-weight preparations. The discrepancies between L_{el}^{exp} and L_{el}^{a} at the higher values of C_p were then attributed to so-called 'semidilute' solution properties of the PSS system[7,9] that are not accounted for in the Odijk model. This interpretation, however, is in contradiction to the Witten–Pincus model[10] for semidilute solutions that was proposed to explain the *increase* in the reduced viscosity upon a *decrease* in the segment concentration. In this model the presence of other chains increases the *screening* of intracharge interactions, thus leading to a *reduction* in the effective persistence length with *increasing* polyion concentration.

It is noted that both Manning condensation and the expression for L_{el}^{a} assume a two-region model for the counterion distribution. That is, the counterions are either tightly bound to the surface of the polyion or uniformly distributed throughout the remaining solution. It is well known, however, that the counterions are not uniformly distributed in a radial direction from the polyion surface. For example, Monte Carlo calculations reported by Le Bret and Zimm[11] indicate that there is a substantial differential in the counterion concentration as one proceeds from the surface of a cylinder into the bulk solution, a gradient that may extend beyond 50 Å. This 'counterion sheath' of several ångströms in thickness can have a profound influence on the flexible nature of the polyions as a function of the ionic strength.

We examine in this paper the properties of a two-region and three-region distribution of counterions on the ionic strength dependence of L_{el}. Previously described exact numerical methods of computing the electrostatic persistence length[12,13] are employed in this analysis. The persistence length obtained in this manner is denoted by L_{el}^{n}, and is referred to as the 'numerical model'.

NUMERICAL MODEL

According to Yamakawa[14], the average energy of bending, $\langle E_b\rangle$, for a linear flexible polymer is related to the elastic bending constant, γ_b, by the expression:

$$\langle E_b\rangle=\frac{1}{2}\left\langle\int_0^L \gamma_b(\partial^2\boldsymbol{r}/\partial s^2)^2\,\mathrm{d}s\right\rangle \tag{7}$$

where $\boldsymbol{r}$ is a point along the polymer and s is the distance of that point along the contour length of the chain. In the spirit of equation (1), we have:

$$\langle E_b\rangle=\left\langle(\gamma_{in}/2)\int_0^L(\partial^2\boldsymbol{r}/\partial s^2)^2\,\mathrm{d}s\right\rangle + \left\langle\frac{1}{2}\int_0^L\gamma_{el}(\partial^2\boldsymbol{r}/\partial s^2)^2\,\mathrm{d}s\right\rangle \tag{8}$$

where γ_{in} is assumed to be independent of curvature as it acts along the contour length of the polyion, whereas the electrostatic interaction acts directly from the space separating the charges and thus γ_{el} may depend upon $\partial^2\boldsymbol{r}/\partial s^2$ (refs. 12 and 13).

For a string of $N+1$ equally spaced beads that undergoes a continuous bend, the line connecting beads 1 and $N+1$ is the chord for an arc of angle $\theta=2\phi$ associated with a circle of radius $R_c=Nb/\theta$. The spatial distance between the ith and jth bead is the chord length for an angle $|i-j|\phi/N$, i.e. $b'_{ij}=(bN/\phi)\sin(|i-j|\phi/N)$. These parameters are illustrated in *Figure 2*.

For a screened Coulombic interaction between 'effective' charges on each group, z_{eff}, one has:

$$E_{el}(\theta)=(A\phi/N)\sum_{j=1}^{N}(N+1-j) \times\exp[-(bN/\phi\lambda_{DH})\sin(j\phi/N)]/[b\sin(j\phi/N)] \tag{9}$$

where $A=[(ez_{eff})^2/\varepsilon]$. If $\partial^2\boldsymbol{r}/\partial s^2=1/R_c=$constant, then:

$$\gamma_{el}=2[E_{el}(\theta)-E_{el}(0)]\Big/\int_0^L(1/R_c)^2\,\mathrm{d}s =2[E_{el}(\theta)-E_{el}(0)]R_c^2/L \tag{10}$$

and the electrostatic persistance length for the *numerical model* is defined as:

$$L_{el}^{n}=\gamma_{el}/kT=2[E_{el}(\theta)-E_{el}(0)]R_c^2/LkT \tag{11}$$

To ensure that intermolecular interactions do not play

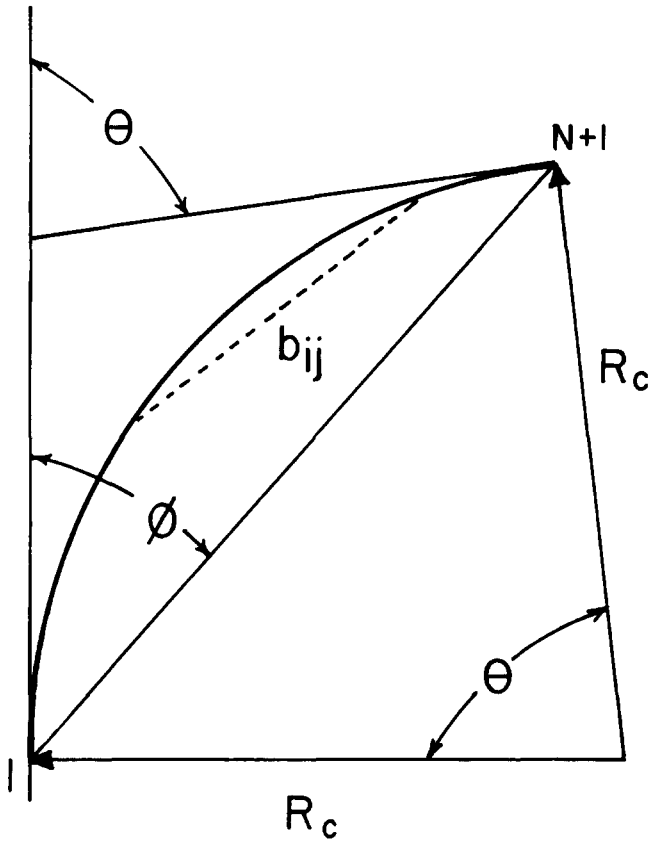

Figure 2 Schematic diagram of parameters for the numerical model

a major role in the analysis, the ion atmosphere associated with neighbouring polyions must not significantly overlap. For simplicity we examine the relative volumes associated with a cylindrical monomeric unit of length $\langle b_{eff}\rangle$ and unit charge along the polymer backbone. It is assumed that the radius associated with the ion cloud surrounding the monomer unit is proportional to the Debye–Hückel screening radius:

$$r_{ic} = \beta_{ic}\lambda_{DH} \tag{12}$$

where β_{ic} is a proportionality constant. Hence the volume of the ion cloud about the monomer unit is:

$$V_{ic} = \pi(\beta_{ic}\lambda_{DH})^2\langle b_{eff}\rangle \tag{13}$$

The solution volume available for each monomer unit is defined as $V_m = 1000/N_A C_p$. Since not all of the monomeric units may be charged due to Manning-type condensation, the effective volume associated with the cylindrical subunit is given by:

$$V_{eff} = V_m/\alpha = \pi\langle b_{eff}\rangle R_{eff}^2 \tag{14}$$

where R_{eff} is the radial extension from the polymer backbone. In the case of zero added salt, $C_s = 0$ in equation (6), and one has for the ratio V_{ic}/V_{eff}:

$$V_{ic}/V_{eff} = \beta_{ic}^2\langle b_{eff}\rangle/4\lambda_B \tag{15}$$

It is clear that if Manning condensation occurs in which $\langle b_{eff}\rangle = \lambda_B$, then $\beta_{ic} \leqslant 2$ in order for the neighbouring polyions to behave independently of each other in the absence of added electrolyte. It is noted from equation (15) that the ratio V_{ic}/V_{eff} is independent of C_p, and thus is also independent of dilution.

Two-region system

The two-region system assumes that the counterions are either condensed on the surface of the polyion or are uniformly distributed throughout the remaining solution. The Debye–Hückel screening length for all pairwise interactions along the isolated chain is therefore computed from equations (3) and (6), where Manning condensation is assumed.

Three-region system

The basis of the three-region system is the Monte Carlo calculations of Le Bret and Zimm[11], which are used as a guide for the radial distribution of counterions about a cylinder, and of Zimm and Le Bret[15], who used the Poisson–Boltzmann equation to examine the effect of geometry on the distribution of counterions. These calculations were carried out with the constraint $10\ \text{Å} = a + r_c$, where r_c is the radius of the cylinder and a is the radius of the counterion. It was reported that for the rod geometry there is a fraction of residual counterions that cannot be diluted away, which they state corresponds to Manning condensation[15]. In the present model it is assumed that these 'bound' counterions act simply to reduce the surface charge of the polyion, and thus define region 1 of the three-region system. The effective charge for each subunit of charge z_p in the polyion is therefore:

$$z_{eff} = z_p(b/\langle b_{eff}\rangle) \tag{16}$$

The two remaining regions for counterion occupation are associated with the distribution of counterions in solution. According to Le Bret and Zimm[11] for the case $a = 1$ Å, the counterion distribution was found to follow closely the Boltzmann distribution law:

$$C_c(r) = C_b \exp[\langle\phi(r)\rangle] \tag{17}$$

where $\langle\phi(r)\rangle$ is the average reduced potential and C_b is the 'bulk', or 'background', counterion concentration. One may therefore approximate the radial density function $\rho(r)$ by:

$$\rho(r) = \Delta\rho_0 \exp(-\gamma r) + \rho_b(\lambda_{DH}) \tag{18}$$

where $\rho_b(\lambda_{DH})$ is the 'background' counterion density whose value depends upon the ionic strength of the solution, $\Delta\rho_0 = \rho_0 - \rho_b(\lambda_{DH})$ is the 'excess' counterion density and γ is a measure of the rate of decay of the distribution function with distance.

In order for $\rho_b(\lambda_{DH})$ to attain a constant value over a finite distance it is necessary that $\lambda_{DH} < R_{eff}$. If $\rho(r)$ decays to $\rho_b(\lambda_{DH})$ within the distance R_{eff}, then $\rho(r)$ is normalized in accordance with the expression:

$$\langle b_{eff}\rangle \int_0^{R_{eff}} \rho(r) 2\pi r\, dr = \alpha C_p V_{eff} = 1 \tag{19}$$

Substitution of equation (18) into equation (19) and subsequent rearrangement gives:

$$2\langle b_{eff}\rangle \Delta\rho_0 \pi \int_0^{R_{eff}} \exp(-\gamma r) r\, dr = 2V_\gamma \Delta\rho_0 H(y) = 1 - f_b(\lambda_{DH}) \tag{20}$$

where

$$H(y) = 1 - \exp(-y)(y+1) \tag{21}$$

$V_\gamma = \pi\langle b_{eff}\rangle/\gamma^2$, $y = \gamma R_{eff}$ and $f_b(\lambda_{DH}) = \rho_b(\lambda_{DH})V_{eff}$ is the

fraction of counterions that represent the baseline of the distribution. The left-hand side of equation (20) is partitioned into two additional regions: region 2 is defined as a 'counterion sheath' in the vicinity of the surface of the cylindrical polyion, and region 3 is defined as the remainder of the solution that extends to R_{eff}. Following the discussion associated with equations (12)–(15), the radius associated with the 'counterion sheath' is $r_{cs}=\beta_{cs}\lambda_{DH}$. Hence by analogy with equation (15):

$$(r_{cs}/R_{eff})^2=\beta_{sc}^2\langle b_{eff}\rangle/4\lambda_B \quad (22)$$

where β_{sc} can be any value over the range $0<\beta_{cs}\leqslant\beta_{ic}$. The average fraction of counterions in region 2 *above the bulk value* is thus given by:

$$2\langle b_{eff}\rangle\Delta\rho_0\pi\int_0^{r_{cs}}\exp(-\gamma r)r\,dr=2\Delta\rho_0V_\gamma H(x)=f_2 \quad (23)$$

where $x=\gamma r_{cs}$ and $H(x)$ is defined by equation (21). The fraction of counterions *above the bulk value* in region 3 is:

$$2\langle b_{eff}\rangle\Delta\rho_0\pi\int_{r_{cs}}^{R_{eff}}\exp(-\gamma r)r\,dr=2\Delta\rho_0V_\gamma[H(y)-H(x)]=f_3 \quad (24)$$

The concentration of counterions in region 2 is thus:

$$C_2=(f_2/V_2)+[f_b(\lambda_{DH})/V_{eff}] \quad (25)$$

and for region 3:

$$C_3=(f_3/V_3)+[f_b(\lambda_{DH})/V_{eff}] \quad (26)$$

with $V_3=V_{eff}-V_2$. The effective counterion concentration between the ith and jth charged groups, C_{ij}, is assumed to be a 'length weighted average' of the concentrations in regions 2 and 3:

$$C_{ij}=X_2C_2+X_3C_3 \quad (27)$$

where $X_k=L_k/b_{ij}$ $(k=1, 2)$, $L_2+L_3=b_{ij}$, and L_2 and L_3 are the total lengths of the line b_{ij} that lie in regions 2 and 3, respectively. Using the identity defined by equation (19), solving for ρ_0V_γ in equation (20) and combining equations (25)–(27) gives for the concentration ratio $C_{ij}/\alpha C_p$:

$$C_{ij}/\alpha C_p=f_b(\lambda_{DH})+[1-f_b(\lambda_{DH})]\{X_2B(x,y)w^2+X_3[w^2/(w^2-1)][1-B(x,y)]\} \quad (28)$$

where $B(y, y)=H(x)/H(y)$ and $w=R_{eff}/r_{cs}=y/x$.

The relative probability for a polyion to bend through an angle θ relative to that of a rod configuration ($\theta=0$) is given by:

$$P(\theta)/P(0)=\exp\{-[E_{el}(\theta)-E_{el}(0)]/kT\} \quad (29)$$

COMPUTATIONAL PARAMETERS

The objective of the present paper is to show that the C_p dependence of L_{el} reported by Weill and Maret[7] is consistent with current ideas regarding the counterion distribution about linear polyions without having to invoke 'semidilute' solution conditions concomitant with 'non-Manning-type condensation'. Calculations using the 'three-region' model are therefore restricted to a single set of parameters to illustrate this point. A more detailed analysis of the 'three-region' model is to be reported elsewhere[16].

As noted in the discussion of equation (15), the parameter β_{ic} that is associated with a charged subunit must be less than 2 in order to ensure that the counterion atmospheres do not overlap. Unfortunately β_{ic} is not a parameter that is under experimental control. We therefore assume a cell model similar to that employed by others in which the overlap of ion atmospheres is negligible. Focus is then given on only the intramolecular contributions to L_{el}. The degree to which the 'excess counterion concentration' extends beyond the surface of the charged cylindrical surface depends upon the value of γ. In the present set of calculations the value $y=\gamma R_{eff}=8$ was chosen because equation (21) gives the value $H(y)=0.997$, or less than 1% error in regard to 'non-overlap' conditions of the adjacent 'excess counterion concentration'.

Since γR_{eff} was chosen to be constant, it follows that $1/\gamma$ is proportional to λ_{DH} and that the relative volumes of regions 2 and 3 are independent of λ_{DH}. In order to adjust the relative concentrations in these two regions upon dilution, the background concentration of counterions must be a function of λ_{DH}. It is assumed that $f_b(\lambda_{DH})$ is a modified form of the Debye–Hückel screening function:

$$f_b(\lambda_{DH})=1-A\exp(-r_0/\lambda_{DH}) \quad (30)$$

where $1\geqslant A\geqslant 0$ and r_0 is a constant 'characteristic length' that determines the rate at which the background concentration of counterions decreases with ionic strength. Hence the limits of $f_b(\lambda_{DH})$ are: 1 as $\lambda_{DH}\to 0$ and $(1-A)$ as $\lambda_{DH}\to\infty$. Note that if $A<1$ then the $\lambda_{DH}\to\infty$ limit means that there is a fraction A of counterions that cannot be diluted from region 2. While this restriction appears to be consistent with the calculations of Zimm and Le Bret[15], there is a major difference in the physical interpretations of these 'bound' counterions. In the present model Manning condensation has already been taken into account by the *reduction* of the charge density along the polyion backbone. The fraction A of 'bound' counterions are confined to region 2 and serve to 'screen' the effective charged units along the polyion backbone.

Calculations for the three-region model were carried out with the parameters $x=2$, $y=8$, $A=0.1$ and $r_0=30$ Å. A representation of the three-region model employed in these calculations is given in *Figure 3*, and the calculation of the effective concentration of the linear weighted concentration given by equation (27) is schematically represented in *Figure 4*.

Manning-type condensation can be taken into consideration in two ways: *method 1* assumes that the charges of $z_{eff}=1$ are separated by an effective distance $\langle b_{eff}\rangle=\lambda_B$; and *method 2* assumes a reduced charge on each group in accordance with equation (16) while maintaining the actual charge spacing b.

It is assumed that the actual molecular parameters for PSS are $\alpha=0.36$, $b=2.7$ Å and the monomer molecular weight of 209. The PSS parameters for the method 1 calculations are: $z_{eff}=1$, $\langle b_{eff}\rangle=7.18$ Å (λ_B for water at 20°C) and the number of charged groups is $N+1=n_s=\alpha M_p/209=26$, 69 and 240, corresponding to the molecular weights $M_p=15\,000$, 40 000 and 140 000, respectively. The PSS parameters for the method 2 calculations are: $z_{eff}=0.38$, $b=2.7$ Å and $n_s=M_p/209=$

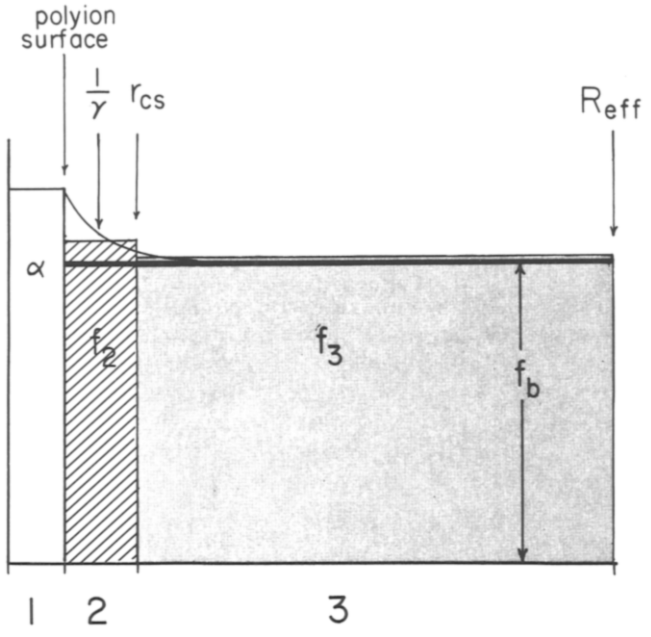

Figure 3 Schematic diagram of the three-region model. The small ion distribution about the cylindrical axis of the polyion is assumed to decay spatially as an exponential function to the bulk solution concentration. The three regions are: region 1, Manning condensation on the surface of the linear polyion with a degree of dissociation α; region 2, a step function representation of the 'counterion sheath' of radius r_{cs} containing the fraction f_2 of counterions; and region 3, a step function representation of the remainder of the solution between polyions, containing the fraction f_3 of counterions. The parameter γ is the rate of spatial decay of the exponential distribution function. The baseline fraction of counterions is denoted by f_b

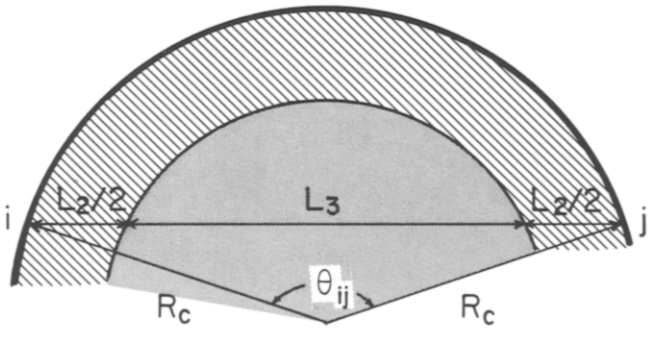

Figure 4 Schematic representation of the effective ionic strength between two charged groups. L_2 is the total distance within the counterion sheath and L_3 is the total distance in the bulk solution for charged groups i and j and an angle θ_{ij} as measured from the centre of a circle of radius R_c

70, 186 and 648, corresponding to $M_p = 15\,000$, 40 000 and 140 000, respectively.

The values of λ_{DH} used in these calculations were the values reported by Weill, Maret and Odijk[9]: λ_{DH} (Å) = 24, 34, 48, 68, 76, 96 and 108.

RESULTS

The ratio L_{el}^n/L_{el}^a for the two-region model for selected values of the bending angle θ at the reported values of λ_{DH} are given in *Table 1* for method 1 calculations and *Table 2* for method 2 calculations.

A somewhat unexpected result of these calculations is that the analytical form L_{el}^a given by equation (2) is quite accurate over a large range of bending angles even though it was derived under the assumption of small deviations from the rod-like configuration. It is also clear from *Tables 1* and *2* that calculations using method 2 provide better agreement with the analytical expression than method 1 for short chains.

The ratio L_{el}^n/L_{el}^a for the three-region model is given in *Table 3* for method 1 calculations and *Table 4* for method 2 calculations. Although the values of L_{el}^n/L_{el}^a are less than unity in these sets of calculations, this ratio can be made greater than unity by decreasing the value of x (ref. 16). This is due to the fact that smaller values of x result in more counterions being partitioned from region

Table 1 L_{el}^n/L_{el}^a: method 1 for two-region model ($\langle b_{eff} \rangle = 7.18$ Å and $z_{eff} = 1$)

		θ (deg)				
n_s	λ_{DH}	20	60	100	140	180
26	24	1.06	1.07	1.09	1.13	1.19
	34	1.07	1.08	1.11	1.16	1.23
	48	1.08	1.10	1.13	1.18	1.25
	68	1.10	1.11	1.14	1.19	1.26
	76	1.10	1.11	1.14	1.19	1.26
	96	1.11	1.12	1.15	1.19	1.26
	108	1.11	1.12	1.15	1.19	1.26
69	24	1.01	1.02	1.02	1.03	1.04
	34	1.02	1.02	1.03	1.04	1.05
	48	1.02	1.03	1.04	1.07	1.10
	68	1.02	1.03	1.05	1.09	1.15
	76	1.02	1.04	1.06	1.10	1.16
	96	1.03	1.04	1.07	1.11	1.17
	108	1.03	1.04	1.07	1.11	1.18
240	24	1.00	1.00	1.00	1.00	1.00
	34	1.00	1.00	1.00	1.01	1.01
	48	1.00	1.00	1.01	1.01	1.01
	68	1.00	1.01	1.01	1.01	1.02
	76	1.00	1.01	1.01	1.02	1.02
	96	1.01	1.01	1.01	1.02	1.04
	108	1.01	1.01	1.02	1.03	1.04

Table 2 L_{el}^n/L_{el}^a: method 2 for the two-region model ($b = 2.7$ Å and $z_{eff} = 0.38$)

		θ (deg)				
n_s	λ_{DH}	20	60	100	140	180
70	24	1.02	1.03	1.05	1.08	1.14
	34	1.03	1.04	1,06	1.10	1.17
	48	1.03	1.04	1.07	1.11	1.18
	68	1.04	1.05	1.07	1.12	1.18
	76	1.04	1.05	1.07	1.12	1.18
	96	1.04	1.05	1.08	1.12	1.17
	108	1.04	1.05	1.08	1.11	1.17
186	24	1.01	1.01	1.01	1.02	1.03
	34	1.01	1.01	1.02	1.03	1.05
	48	1.01	1.01	1.03	1.05	1.09
	68	1.01	1.02	1.04	1.07	1.13
	76	1.01	1.02	1.04	1.08	1.14
	96	1.01	1.02	1.05	1.09	1.15
	108	1.01	1.02	1.05	1.09	1.15
648	24	1.00	1.00	1.00	1.00	1.00
	34	1.00	1.00	1.00	1.00	1.01
	48	1.00	1.00	1.00	1.01	1.01
	68	1.00	1.00	1.01	1.01	1.02
	76	1.00	1.00	1.01	1.01	1.02
	96	1.00	1.00	1.01	1.02	1.03
	108	1.00	1.01	1.01	1.02	1.04

Table 3 L_{el}^{n}/L_{el}^{a}: method 1 for the three-region model ($\langle b_{eff}\rangle = 7.18$ Å, $z_{eff}=1$, $x=2$, $y=8$, $A=0.1$, $r_0=30$ Å)

			θ (deg)				
n_s	λ_{DH}	f_b	20	60	100	140	180
26	24	0.97	0.89	0.92	0.97	1.04	1.11
	34	0.96	0.88	0.90	0.96	1.03	1.11
	48	0.95	0.89	0.90	0.95	1.02	1.10
	68	0.94	0.93	0.94	0.97	1.02	1.10
	76	0.93	0.94	0.96	0.98	1.03	1.10
	96	0.93	0.98	0.99	1.01	1.05	1.12
	108	0.92	0.99	1.00	1.03	1.07	1.13
69	24	0.97	0.83	0.83	0.86	0.88	0.91
	34	0.96	0.77	0.79	0.82	0.87	0.92
	48	0.95	0.74	0.76	0.82	0.88	0.94
	68	0.94	0.73	0.76	0.82	0.89	0.96
	76	0.93	0.74	0.76	0.82	0.89	0.96
	96	0.93	0.75	0.76	0.82	0.90	0.97
	108	0.92	0.76	0.77	0.83	0.90	0.98
240	24	0.97	0.81	0.81	0.81	0.81	0.81
	34	0.96	0.75	0.75	0.75	0.75	0.76
	48	0.95	0.70	0.70	0.70	0.72	0.73
	68	0.94	0.66	0.67	0.68	0.70	0.73
	76	0.93	0.66	0.66	0.68	0.70	0.74
	96	0.93	0.64	0.65	0.67	0.71	0.75
	108	0.92	0.64	0.65	0.68	0.72	0.77

Table 4 L_{el}^{n}/L_{el}^{a}: method 2 for the three-region model ($\langle b_{eff}\rangle = 2.7$ Å, $z_{eff}=0.38$, $x=2$, $y=8$, $A=0.1$, $r_0=30$ Å)

			θ (deg)				
n_s	λ_{DH}	f_b	20	60	100	140	180
70	24	0.97	0.86	0.89	0.94	0.99	1.06
	34	0.96	0.84	0.86	0.91	0.98	1.05
	48	0.95	0.85	0.86	0.90	0.96	1.04
	68	0.94	0.88	0.89	0.91	0.96	1.03
	76	0.93	0.89	0.90	0.92	0.97	1.03
	96	0.93	0.91	0.92	0.95	0.98	1.04
	108	0.92	0.93	0.94	0.96	1.00	1.05
186	24	0.97	0.82	0.83	0.85	0.88	0.90
	34	0.96	0.77	0.78	0.82	0.86	0.90
	48	0.95	0.73	0.75	0.80	0.86	0.92
	68	0.94	0.72	0.74	0.80	0.87	0.94
	76	0.93	0.72	0.74	0.81	0.87	0.95
	96	0.93	0.74	0.75	0.81	0.88	0.95
	108	0.92	0.75	0.76	0.81	0.88	0.95
648	24	0.97	0.81	0.81	0.81	0.81	0.81
	34	0.96	0.75	0.75	0.75	0.75	0.76
	48	0.95	0.70	0.70	0.70	0.71	0.73
	68	0.94	0.66	0.66	0.68	0.70	0.73
	76	0.93	0.65	0.66	0.67	0.70	0.73
	96	0.93	0.64	0.65	0.67	0.71	0.75
	108	0.92	0.64	0.64	0.67	0.72	0.76

2 to region 3, thus approaching the two-region model in the asymptotic limit $x \to 0$. (Recall that the choice of $x=2$ in the present three-region calculations is based on the *trend* of L_{el} on λ_{DH} for PSS as reported by Weill, Maret and Odijk[9] and not on the *magnitude* of these data.)

It is clear from the three-region calculations that the value of L_{el}^{n} depends more strongly on the value of the bending angle than for the two-region model. This increased sensitivity of L_{el}^{n} on λ_{DH} is a direct result of the variable concentration C_{ij} between the two pairs of charged groups. To construct the L_{el}^{n}/L_{el}^{a} *versus* λ_{DH} plot to compare with the experimental results summarized in *Figure 1*, we examine the probability of bending through an angle θ relative to the rod-like configuration. This is to ensure that the probability of occurrence is virtually the same for all values of L_{el}^{n}. Selected values of $P(\theta)/P(0)$ for the three chain lengths are given in *Table 5*. Clearly $P(20°)/P(0)>0.98$ for all values of n_s; hence the values of L_{el}^{n} calculated at $\theta=20°$ were used in the L_{el}^{n}/L_{el}^{a} *versus* λ_{DH} plots given in *Figure 5*.

DISCUSSION

It is clear from the comparisons made in *Tables 1* and *2* that the Odijk[1] formulation of L_{el}^{a} given by equation (2) compares well with the exact numerical evaluation of L_{el}^{n}, even for deviations substantially removed from a rod-like configuration. This means that the deviations of L_{el}^{exp}/L_{el}^{a} from unity as shown in *Figure 1 are not due to the mathematical approximations* intrinsic to the derivation

Table 5 $P(\theta)/P(0)$ for two- and three-region models[a]

			θ (deg)				
n_s	λ_{DH}	f_b	20	60	100	140	180
70	24	0.97	0.9963	0.9661	0.9037	0.8107	0.6910
	24	1.00	0.9956	0.9607	0.8928	0.7951	0.6721
	68	0.94	0.9883	0.8980	0.7358	0.5300	0.3247
	68	1.00	0.9861	0.8806	0.6963	0.4782	0.2753
	108	0.92	0.9842	0.8654	0.6628	0.4330	0.2322
	108	1.00	0.9824	0.8505	0.6312	0.3928	0.1969
186	24	0.97	0.9983	0.9843	0.9558	0.9126	0.8554
	24	1.00	0.9979	0.9808	0.9475	0.8990	0.8372
	68	0.94	0.9910	0.9194	0.7768	0.5853	0.3839
	68	1.00	0.9874	0.8912	0.7217	0.5169	0.3181
	108	0.92	0.9831	0.8559	0.6288	0.3745	0.1716
	108	1.00	0.9772	0.8105	0.5500	0.2958	0.1185
648	24	0.97	0.9995	0.9951	0.9865	0.9736	0.9566
	24	1.00	0.9993	0.9939	0.9833	0.9675	0.9467
	68	0.94	0.9967	0.9704	0.9184	0.8417	0.7436
	68	1.00	0.9950	0.9556	0.8811	0.7795	0.6607
	108	0.92	0.9925	0.9338	0.8194	0.6607	0.4831
	108	1.00	0.9882	0.8985	0.7414	0.5527	0.3694

[a] Method 2 calculations with model parameters given in *Tables 3* and *4*

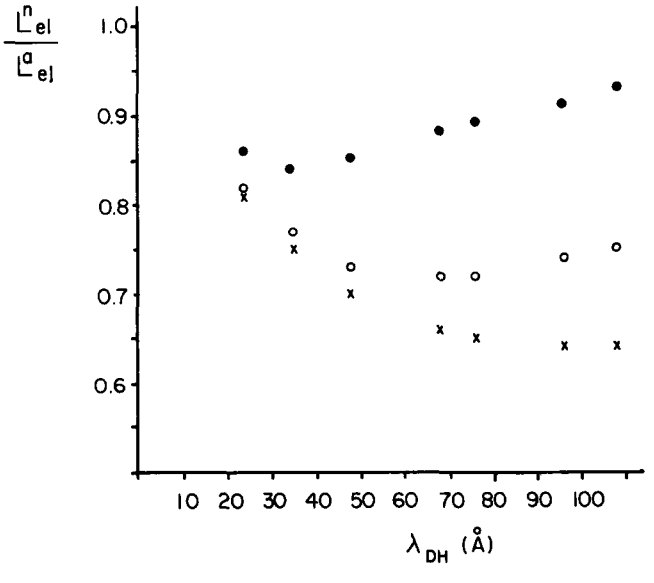

Figure 5 L_{el}^{n}/L_{el}^{a} *versus* λ_{DH} for the three-region model. The set of arbitrary parameters used in these calculations were: $x=2$, $y=8$, $b=2.7$ Å, $z_{eff}=0.38$, $A=0.1$, $r_0=30$ Å, and $n_s=70$ (●), 186 (○) and 648 (×)

of equation (2). The explanation must therefore lie in the phenomena not considered in the Odijk model.

Weill, Maret and Odijk[9] attempted to circumvent the problem by invoking 'semidilute' solution conditions on the higher molecular-weight preparations. In order for this interpretation to be viable, however, they had to impose a different degree of counterion condensation for the higher molecular-weight preparations ($I_s = 0.36C_p$) than for the lower molecular-weight preparations ($I_s = 0.18C_p$). In making this assumption the L_{el}^{exp}/L_{el}^{a} *versus* λ_{DH} curves were shifted to higher values of L_{el}^{exp}/L_{el}^{a} and lower values of λ_{DH}. The result was values of L_{el}^{exp}/L_{el}^{a} that were greater than unity for values of $\lambda_{DH} < 50$ Å. Hence the effect of 'chain overlap' is to 'stiffen' L_p and therefore give a much larger value for L_{el}^{exp} if L_{in} is assumed unchanged. This argument is untenable because: (1) it makes an unwarranted assumption that the *degree* of counterion condensation is chain-length-dependent, a position not supported by other experimental data; (2) it requires that *short* chains are more efficient in causing counterion condensation than the long chains, thereby inferring that long chains become 'stiffer' than short chains as the ionic strength is lowered; and (3) it requires that the semidilute solution effects on L_p act in a direction opposite to that for neutral polymers, the latter being manifested as the presence of *faster* 'collective modes' that result from chain–chain contact points.

It is suggested in this paper that the discrepancy between L_{el}^{exp} and L_{el}^{a} lies mainly in the basic assumption of a statistically uniform distribution of intervening small ions between any two pairs of charged groups on the linear polyion. As illustrated in *Figure 5*, the ratio L_{el}^{exp}/L_{el}^{a} based on the three-region model mimics the λ_{DH} dependence of experimental data given in *Figure 1* for the three molecular weights examined. The discrepancy in the magnitudes of these two sets of data is partially overcome by taking into consideration the *angle averaged* value of L_{el}^{n}/L_{el}^{a}:

$$\langle L_{el}^{n}/L_{el}^{a}\rangle = \frac{\sum [P(\theta)/P(0)][L_{el}^{n}(\theta)/L_{el}^{a}]}{\sum [P(\theta)/P(0)]} = \frac{\sum P(\theta)[L_{el}^{n}(\theta)/L_{el}^{a}]}{\sum P(\theta)} \quad (31)$$

since $P(0)$ is constant. To illustrate we use the values given in *Tables 4* and *5* for the five values of θ. For $n_s = 70$ and $\lambda_{DH} = 24$ Å, one calculates from equation (31) the value $\langle L_{el}^{n}/L_{el}^{a}\rangle = 0.93$, which compares with the value of $L_{el}^{n}/L_{el}^{a} = 0.86$ at $\theta = 20°$ that appears in the plot given in *Figure 5*. The reason that L_{el}^{n} increases as one departs from a rod-like configuration is due to two primary factors: (1) the interaction between two charges acts directly through the solution and not along the chain contour, hence the interaction between these two groups initially increases as the linear polyion is bent; and (2) the 'effective' intervening ionic strength initially decreases due to the relative weighting factors X_2 and X_3 in equation (27). It is noted, however, that under certain conditions L_{el}^{n} for the three-region model may actually decrease as θ is further increased due also to the relative weighting factors X_2 and X_3 (ref. 16).

It is of interest to note that long chains may actually become 'more stiff' than short chains as the ionic strength is lowered. Although this conclusion was drawn from objection (2) to the Weill, Maret and Odijk[9] interpretation given above, the reason for the 'inverse chain stiffening' lies not in differential condensation of short and long chains but rather in the cumulative electrostatic requirement for a screened Coulombic potential. To illustrate, let us assume that we are located at the jth charged group in the chain. As the ionic strength is lowered, the force exerted by other charged groups increases due to two effects. First, the existing interactions are increased due to the reduced screening effect of a smaller number of intervening ions. Secondly, more groups become 'visible' to the jth group through new electrostatic interactions that result from the reduced number of intervening ions. For short chains, however, the number of 'new groups' rapidly becomes depleted and any additional force exerted on the jth group must come solely from an increase in the existing interactions. Owing to the damped nature of a screened Coulombic interaction, the *range of significant increments to the interaction energy* (relative to kT) is somewhat limited. As a result, the short chains become less sensitive to further decreases in the ionic strength than do the larger chains. This type of behaviour is manifested in the Odijk expression given by equation (2). Rearrangement of this expression to the form λ_{DH}/L_{el}^{a} *versus* L/λ_{DH} results in a minimum at the value[13] $(\lambda_{DH}/L)_{min} = y_{min} = 4.1155$, or:

$$\lambda_{DH}/L_{el}^{a} = 39.94\langle b_{eff}\rangle^2/\lambda_B L \qquad (\lambda_{DH}/L = 4.1155) \quad (32)$$

The quantity y_{min} is a 'turn-around' value in that the rate of polyion expansion upon increase in λ_{DH} is governed more by the function $h(Y)$ than λ_{DH}^2 in equation (2). It is also evident that flexible chains *never achieve a fully expanded rod-like configuration*, even if $L < \lambda_{DH}$.

The two conclusions drawn from equation (2), i.e. that short chains may be more flexible than longer chains and that flexible chains do not achieve 'extended-rod status', are consistent with recent viscosity measurements on PSS in the absence of added salt as reported by Yamanaka *et al.*[17]. The viscosity data were obtained with three types of viscometers (Ubbelohde, precision rotational and variable shear viscometers) under nitrogen atmosphere conditions to minimize contamination by dissolved CO_2. These authors stated that the relative viscosity of their lowest molecular-weight sample ($\langle M_w\rangle = 3.7 \times 10^5$) was significantly lower than for the other samples. This observation can be explained if the lower-weight sample was more flexible than the other samples under identical ionic strength conditions. Data on the remaining samples for the intrinsic viscosity ($[\eta] = KM^a$) gave a power law of $a = 1.2$, which is significantly smaller than the expected value of $a = 2$ if the PSS was fully extended.

CONCLUSIONS

It is concluded that the three-region model provides a more viable explanation for the L_{el}^{exp}/L_{el}^{a} *versus* λ_{DH} data on PSS of Weill and Maret[7] than the 'semidilute' solution interpretation of Weill, Maret and Odijk[9]. This assertion is based on the observation that the three-region model is consistent with current thoughts on the distribution of small ions in the vicinity of the polyions, and that short and long chains are treated equally in regard to the degree of counterion concentration. It is also concluded that very flexible polyions with screened Coulombic intrachain interactions *never* achieve rigid-rod status regardless of the value of the ratio L/λ_D. Hence there is no 'coil-to-rod' transition for these flexible coils,

although the coils can become highly extended at the lower ionic strength solutions.

REFERENCES

1 Odijk, T. *J. Polym. Sci., Polym. Phys. Edn.* 1977, **15**, 477
2 Skolnick, J. and Fixman, M. *Macromolecules* 1977, **10**, 944
3 Manning, G. S. *J. Chem. Phys.* 1969, **51**, 924
4 Manning, G. S. *Biophys. Chem.* 1977, **7**, 95
5 Manning, G. S. *J. Am. Chem. Soc.* 1979, **12**, 443
6 Odijk, T. and Houwaart, A. C. *J. Polym. Sci., Polym. Phys. Edn.* 1978, **16**, 627
7 Weill, G. and Maret, G. *Polymer* 1982, **23**, 1990
8 Weill, G. and Maret, G. *Biopolymers* 1983, **22**, 2727
9 Weill, G., Maret, G. and Odijk, T. *Polym. Rep.* 1984, **25**, 147
10 Witten, T. A. and Pincus, P. *Europhys. Lett.* 1987, **3**, 315
11 Le Bret, M. and Zimm, B. H. *Biopolymers* 1984, **23**, 271
12 Schmitz, K. S. and Yu, J.-W. *Macromolecules* 1988, **21**, 484
13 Schmitz, K. S., 'An Introduction to Dynamic Light Scattering by Macromolecules', Academic Press, Boston, 1990
14 Yamakawa, H., 'Modern Theory of Polymer Solutions', Harper and Row, New York, 1971
15 Zimm, B. H. and Le Bret, M. *J. Biomol. Struct. Dynam.* 1983, **1**, 461
16 Klearman, D. and Schmitz, K. S. 'Photon Correlation Spectroscopy: Multicomponent Systems' SPIE Conference Proceedings, January 1991, in press
17 Yamanaka, J., Matsuoka, H., Kitano, H., Hasegawa, M. and Ise, N. *J. Am. Chem. Soc.* 1990, **112**, 587